**Integration of pathway, cellular and genetic context reveals principles of synthetic lethality that affect reproducibility**

Angel A. Ku[1], Sameera Kongara[1], Hsien-Ming Hu[1], Xin Zhao[1], Di Wu[2], Frank McCormick[2], Allan Balmain[2], Sourav Bandyopadhyay[1,2,*]

[1] Department of Bioengineering and Therapeutic Sciences. University of California, San Francisco. San Francisco, CA

[2] Helen Diller Family Comprehensive Cancer Center. University of California, San Francisco. San Francisco, CA

* Correspondence: Sourav.bandyopadhyay@ucsf.edu

**ABSTRACT**

Synthetic lethal screens have the potential to identify new vulnerabilities incurred by specific cancer mutations but have been hindered by lack of agreement between studies. Using KRAS as a model, we identified that published synthetic lethal screens significantly overlap at the pathway rather than gene level. Analysis of pathways encoded as protein networks identified synthetic lethal candidates that were more reproducible than those previously reported. Lack of overlap likely stems from biological rather than technical limitations as most synthetic lethal phenotypes were strongly modulated by changes in cellular conditions or genetic context, the latter determined using a pairwise genetic interaction map that identified numerous interactions that suppress synthetic lethal effects. Accounting for pathway, cellular and genetic context nominates a DNA repair dependency in KRAS-mutant cells, mediated by a network containing BRCA1. We provide evidence for why most reported synthetic lethals are not reproducible which is addressable using a multi-faceted testing framework.

**STATEMENT OF SIGNIFICANCE**

Synthetic lethal screens have the power to identify new targets in cancer, although have thus far come up short of expectation. We use computational and experimental approaches to delineate principles for identifying robust synthetic lethal targets that could aid in the development of effective new therapeutic strategies for genetically defined cancers.

## INTRODUCTION

Synthetic lethality is a type of genetic interaction that occurs when the simultaneous perturbation of two genes results in cell death. Such an approach has been used to define new vulnerabilities in cancer cells harboring defined mutations, such as the case of BRCA1- or BRCA2- mutant cells which are sensitive to PARP inhibition (Bryant et al., 2005; Farmer et al., 2005). In search of such vulnerabilities, functional genomic screens have enabled the rapid mapping of potential synthetic lethal relationships using isogenic or collections of cell lines harboring specific mutations of interest. Historical screens using RNAi technologies have been widely suggested to suffer from library quality and off target effects that have limited the reproducibility of published synthetic lethal candidates (Downward, 2015; Mullard, 2017). It has been suggested that CRISPR pooled screens may overcome these issues. Another possibility is that the predominant barrier to identifying reproducible synthetic lethals is that of interaction penetrance, or resiliency against modulation by additional genetic changes found in cancers (Ashworth et al., 2011; Ryan et al., 2018). Computational and experimental strategies geared towards resolving and overcoming challenges in synthetic lethal identification are largely unexplored.

KRAS is the most commonly mutated oncogene in cancer. It is as yet undruggable, activates a variety of signaling pathways, and is exemplary to the challenges in identifying synthetic lethals. While a multitude of studies have sought to define KRAS synthetic lethal genes (Costa-Cabral et al., 2016; Kim et al., 2013, 2016; Luo et al., 2009; Scholl et al., 2009; Steckel et al., 2012), they have been notable for the fact that they hardly overlap, which has been attributed to the use of different cell lines and screening libraries that may suffer from off-target effects and partial knockdowns (Downward, 2015). As a result, many of the published synthetic lethal genes that have been explored independently have failed to reproduce (Fröhling and Scholl, 2011; Tessema et al., 2014). While a meta-analysis of published synthetic lethals could be an effective way to identify more robust candidates, a systematic integration and re-testing has not yet been performed (Christodoulou et al., 2017; Downward, 2015).

The bulk of our knowledge of the organization of genetic interactions comes from model organisms through single and combination knockout studies (Rancati et al., 2018). Large scale mapping of such interactions, including synthetic lethals, have been found to link functionally related proteins and used to delineate pathway structure (Collins et al., 2007; Costanzo et al., 2010). Genetic interactions have been shown to be highly context specific with changes in environment and strain dramatically altering pathway usage and synthetic lethal relationships in yeast (Bandyopadhyay et al., 2010; Galardini et al., 2018). The plasticity of genetic interactions present in single-celled organisms likely foreshadows the challenges in the identification of clinically relevant synthetic lethal interactions in a heterogeneous disease such as cancer.

We hypothesized that challenges in identifying synthetic lethal interactions stems from the fact that differences in gene dependencies among cancer cells parallel the widespread differences in gene essentiality observed in model organisms that are exposed to environmental or genetic changes (Galardini et al., 2018; Rancati et al., 2018). Integrating across studies, we show that previously published KRAS synthetic lethal screens contain significant information regarding the pathways required for KRAS mutant cells in a manner that extends beyond the single gene that is often reported. Genes involved in these pathways were more likely to be recapitulated in confirmatory studies, indicating that they are more likely to be context-independent. Further testing of synthetic lethal genes identified that most were profoundly influenced by changes in cellular conditions and presence of genetic modifiers, likely explaining why published synthetic lethals have had limited utility. Accounting for context highlights a DNA repair pathway as a dependency in KRAS mutant cancers, which was reproducibly observed in multiple studies but not always the top hit and therefore not immediately apparent. We delineate why most synthetic lethal interactions are not reproducible, and define a new approach to process and integrate synthetic lethal screens to identify context-independent genetic interactions that operate at the level of a pathway rather than a single gene.

## RESULTS

### Meta-analysis of published KRAS synthetic lethal screens identifies reproducible synthetic lethal networks

The concept of synthetic lethality is a powerful tool to identify new dependencies and gene targets in cancer, but despite their potential their utility has been limited by challenges in robustness and reproducibility related to cellular context (Ashworth and Lord, 2018; Downward, 2015; Lord and Ashworth, 2016; Ryan et al., 2018). We hypothesized that integrating multiple independent studies may reveal synthetic lethal interactions that are independent of cellular context and hence more reproducible. To determine the degree to which this was the case, we analyzed three seminal studies which sought to define KRAS synthetic lethal genes through loss of function screens, hereafter called the Luo, Barbie and Steckel studies (Barbie et al., 2009; Luo et al., 2009; Steckel et al., 2012). The Luo and Steckel studies used unique pairs of isogenic cells whereas the Barbie study used a panel of KRAS mutant and wild-type cell lines. As a basis for comparison we selected the top 250 KRAS synthetic lethal genes reported in each study as hits (KSL genes, Table 1), and found that there was marginal overlap between any pair of studies based on a hypergeometric test accounting for total number of tested genes in each study, consistent with previous reports (Fig. 1A) (Christodoulou et al., 2017; Downward, 2015). We next explored whether each screen could have identified distinct but related genes, indicating shared essentiality at the pathway rather than gene level. For example, different subunits of the 26S proteasome (PSMB6, PSMD14) were identified by different studies (Downward, 2015), suggesting convergence between studies at the pathway level (Fig. 1A). We integrated these gene lists with a protein-protein interaction (PPI) network comprising known protein complexes from CORUM and high confidence physical and functional interactions from HumanNet (Lee et al., 2011; Ruepp et al., 2010). In total we identified 6,830 interactions involving a protein product of a KSL gene from any of the three studies (Fig. 1B). Overall we found 260 interactions connecting KSL genes found in different studies. To assess if this was a significant number we compared the number of interactions spanning between pairs of studies to the number of interactions expected among randomly selected gene sets, controlling for sample size and test space (see

Methods). In all cases, we observed significantly more connections between KSL genes from two independent studies than expected at random (Fig. 1C). For example, we observed 162 PPIs between the top 250 genes in the Luo and Steckel studies, which was approximately 8-fold higher than expected between 250 random genes, representing a $p<0.0001$. In contrast, the gene level overlap between these two studies was not significant ($p=0.17$) (Fig. 1A).

Since KSL genes from different studies were enriched to interact functionally and physically, we next asked if they converge into molecular sub-networks representing known pathways and protein complexes. We applied a network clustering algorithm called MCODE on this network to identify dense gene sub-networks, or modules, enriched with KSL genes spanning multiple studies (Bader and Hogue, 2003). Based on our requirement that a subnetwork must include a gene found in two or more studies, we identified 7 functionally distinct KRAS synthetic lethal networks, all of which could be traced back to a specific protein complex or pathway (Fig. 1D, Table 2A). For example, one of the networks corresponds to the Proteasome and Anaphase promoting complex (CORUM ID: 181 & 96), which includes subunits encoded by genes identified in the Luo, Barbie and Steckel studies (Fig. 1D). Other complexes and pathways we identified in this study were the Nop56p-associated pre-rRNA complex (containing Steckel and Luo genes), BRCA1-RNA polymerase II complex (Steckel and Barbie), the RC complex during S-phase of the cell cycle (all three studies), LCR-associated remodeling complex also called LARC (all three studies), the Chaperonin containing TCP1 complex also called CCT (Luo and Steckel) and the Insulin signaling pathway (Steckel and Barbie). In all cases, these complexes and pathways were significantly enriched for KSL genes (Fig. 1D). In total we predicted 105 KRAS synthetic lethal network genes (Network SL genes), of which 65% (68/105) were not covered in our original KSL lists (Fig. 1D, Table 2, 3). Hence, despite the limited gene level overlap in published studies, network integration reveals that independent KRAS synthetic lethal studies converge on shared protein complexes and pathways.

**KRAS synthetic lethal networks gene are more like to be hits in other published studies**

Since our network analysis highlighted shared pathways and complexes across studies, we hypothesized that Network SL genes may represent synthetic lethals that are more robust, and hence more likely to be reproduced in follow up studies. To address this we asked if they were more likely to be recovered in a series of more recent RNAi screens that were not used for network identification as compared to 26 previously published KRAS synthetic lethal genes curated from the literature (Literature SL) (Table 2B) (Costa-Cabral et al., 2016; Kim et al., 2013, 2016). Both Kim et al. 2013 (Kim et al., 2013) and Kim et al. 2016 (Kim et al., 2016) studies used panels of KRAS mutant versus wild-type lung cancer lines, and the Costa-Cabral study (Costa-Cabral et al., 2016) used an isogenic panel of colorectal cancer lines. To facilitate comparison, we independently ranked genes identified from each of these three studies into percentiles, with genes in the lowest percentile showing the strongest evidence of KRAS synthetic lethality (see Methods). Network SL genes were more likely to be among the top percentile of hits than Literature SL genes previously published. For example, in the Kim et al 2016 study, 15% of the Network SL genes tested were in the top one percentile of hits as compared to 3% of Literature SL genes, a 5-fold increase (Fig. 2). Similarly, 9% of Network SL genes were in the top 1% of hits in the Kim et al. 2013 study, compared to 0% using Literature SL genes. Network SL genes also predicted the top candidate from the Costa-Cabral study, CDK1. Taken together as a meta-analysis of six studies, these data provide additional support for genes involved in the RC complex during S-phase (CDK1, RPA1, RPA2) and the BRCA1-RNA polymerase II complex (POLR2B, POLR2D, POLR2G, BRCA1) as KRAS synthetic lethal candidates that were repeatedly replicated in multiple studies. Hence a network approach to identifying synthetic lethal genes based on their pathway context identifies reproducible synthetic lethals in a manner that is superior to the standard single study, single gene approach.

**Evaluation of published and predicted KRAS SLs in an isogenic KRAS dependency model.**

We next sought to obtain independent experimental evidence that the incorporation of pathway context could identify robust KRAS synthetic lethals. We established an isogenic model using MCF10A cells expressing KRAS G12D or eGFP as control and screened them in parallel using an arrayed gene

knockdown library independently targeting 28 Literature SL genes, 40 Network SL genes and 128 genes in KRAS pathway (Fig. 3A, Supplementary Fig. S1, Table 3). MCF10A cells are non-transformed and have been used extensively to model RAS signaling (Martins et al., 2015; Stolze et al., 2015) and mutant KRAS is often amplified in human cancer, indicating the relevance of our approach (Ding et al., 2008; Modrek et al., 2009). KRAS G12D cells did not proliferate significantly more than control eGFP expressing cells and KRAS cells were growth factor independent and sustained MAPK activity in the absence of growth factor, a hallmark of oncogenic transformation and key feature of KRAS biology (Fig. 3B,C). As positive control, we observed that knockdown of KRAS only reduced the proliferation of KRAS-expressing cells in the absence of all media supplements and growth factors (minimal media), demonstrating KRAS dependency in this model (Fig. 3D). Comparison of the proliferative impact of gene knockdown in control eGFP versus KRAS mutant cells grown in minimal media was used to define an interaction score related to the significance of effect over four replicates, with negative scores representing putative synthetic lethal hits (see Methods). Using a False Discovery Rate (FDR) cutoff of 5%, we identified 28 hits including KRAS (Fig. 3E). Among the top 10 genes were predicted Network SL genes BRCA1 (S=-6.3) and RPA3 (S=-4.2), and previously described Literature SL genes GATA2 (S=-4.9), YAP1 (S=-2.9) and RHOA (S=-5.4) (Fig. 3F). At the pathway level KRAS cells were notably dependent on genes in the RAS, ribosomal protein S6 kinase (S6K), cell cycle and YAP pathway (Fig. 3G). Inhibition of receptor tyrosine kinase (RTK) signaling had the least effect on the KRAS cells, as typified by knockdown of GRB2, which links RTKs and RAS signaling, that was more toxic to eGFP than KRAS cells (S=5.9) (Fig. 3F,G). Most hits were independent of the particular KRAS allele used as screening results between G12V and G12D expressing cells were highly correlated (r=0.81, Supplementary Fig. 2, Table 4). With respect to previously published Literature SL genes, we found that 6/27 (22%) were recovered at an FDR<10% but on average they did not have negative interaction scores consistent with synthetic sickness or lethality as a group (p=0.48 based on Student's t-test) (Fig. 3I). In contrast, the 39 predicted Network SL genes as a group had overall strong negative scores (p=4.6e-5 based on Student's t-test) that were overall more negative than Literature SL genes (p=0.046), and 33% were synthetic lethal hits (13/39 at a FDR of 10%) (Fig. 3I). Taking our

retrospective analysis and new experimental data together, our findings indicate that a network meta-analysis approach is an effective strategy to identify robust and reproducible synthetic lethal genes.

**Dependency of KRAS synthetic lethals on genetic context**

Limitations in gene knockdown technologies have been suggested to contribute to the lack of reproducibility of KRAS synthetic lethals and potentially resolved using CRISPR-based approaches (Downward, 2015). Another explanation could be that synthetic lethal effects are incompletely penetrant and do not manifest equally in cells with different genetic backgrounds (Ryan et al., 2018). To establish the degree to which genetic context influences synthetic lethal identification and to elucidate targets that are resilient to this effect, we systematically screened for secondary perturbations that alter synthetic lethal phenotypes. We generated a quantitative epistasis map (E-MAP) through the systematic measurement and comparative analysis of the fitness of single and pairwise gene perturbations using RNA interference (Roguev et al., 2013). In this system, positive scoring interactions constitute buffering or epistatic interactions and occur when the effect of combination knockdown is less than what is expected given the two gene knockdowns separately, in the extreme case causing a complete suppression of the phenotype of one perturbation by the another (Boone et al., 2007; Guarente, 1993). Negative interactions indicate gene pairs that operate independently and when co-depleted produce a stronger phenotype than expected (Boone et al., 2007). We generated an E-MAP in MCF10A KRAS G12D cells by knocking down the 31 of the top synthetic lethal genes we identified in our single gene study (query genes) in combination with 188 genes mostly involved in the broader RAS signaling pathway (Fig. 4A, Table 5). Together, we measured interactions among 5,828 gene pairs and identified 170 positive and 105 negative interactions at a score cutoff of 2 ($Z>|2|$) corresponding to two standard deviations from the mean (Fig. 5b). At this score cutoff we found strong interactions occurring between 4.6% of gene pairs, consistent with observed genetic interaction rates in yeast (Costanzo et al., 2016).

For the 31 query genes we tested, we identified 170 genetic interactions that suppress their synthetic lethal phenotype in KRAS mutant cells ($Z$>2, average of 5.5 per gene). We validated several of the strongest hits in small-scale studies. For example, while CCND1 knockdown was selectively toxic to KRAS cells, co-knockdown of RASSF5 reverted KRAS mutant cells back to normal proliferation ($Z$=3.9) (Fig. 4C). The impact of knockdown of CDK6 was also significantly rescued by knockdown of RASSF5 ($Z$=3.8) and ERBB2 ($Z$=3.3). Genetic modifiers could also modulate dependency on published KRAS synthetic lethal targets. For example, while knock down of STK33 was selectively toxic in KRAS G12D but not eGFP cells it was suppressed by simultaneous knockdown of SHP2 ($Z$=5.1) or ARID1B ($Z$=3.0) (Fig. 4C). A pathway-based analysis identified 32 connections between query genes and cellular pathways where interactions could be organized as a bundle that were significantly positive or negative (p=0.05, Fig. 4D, see Methods). For example, we identified that knockdown of RALGDS-Like 1 (RGL1) displayed positive interactions with genes involved in stress-linked MAPK, RHO, and RAC pathways (Fig. 4D,E) and found largely negative interactions between DNA Methyltransferase 3 Alpha (DNMT3A) and the spliceosome and anaphase and proteasome complex (Fig. 4E). These results demonstrate that KRAS synthetic lethal gene inhibition may be suppressed by loss of secondary genes and pathways, in some instances completely rescuing lethal phenotypes.

**Dependency of KRAS synthetic lethals on media complexity**

Environmental differences such as variation in the growth factors and nutrients available in serum and media can alter cell biology (McGillicuddy et al., 2018; Stein, 2007) and have been postulated to contribute to challenges in validating candidate therapeutic targets in cancer (Settleman et al., 2018). We postulated that such changes in cellular context may be a potential source of the lack of durability in reported synthetic lethal genes in vitro. If correct, this could be a significant detriment to advancing synthetic lethal targets in vivo and in humans where such variability certainly exists in the complex tumor microenvironment. To model such changes, we iteratively added supplements back into the minimal media that was used in our initial screen to MCF10A KRAS G12D cells. To minimal media we

added insulin, cholera toxin, and hydrocortisone (termed intermediate media) and found that it partially rescued cellular dependency on KRAS and further addition of EGF (full media) completely abolished KRAS dependency (Fig. 5A). We performed parallel single gene knockdown screens using these three different conditions and found dramatic differences in the synthetic lethal interactions we observed (Fig. 5B, Table 4). Strikingly, genetic interaction scores between experiments performed in minimal or intermediate media were weakly correlated and not significant (r = 0.11) (Fig. 5B, Table 4).

We next explored the degree to which media conditions modulate the dependency on published KRAS synthetic lethal genes. We observed that synthetic lethality with members of the proteasome (e.g. PSMA2, PSMA5) (Luo et al., 2009; Steckel et al., 2012) was only evident in cells that were grown in more complex media (and KRAS independent) suggesting that this pathway may only be necessary for KRAS-mutant cells when both KRAS and growth factor signaling are present (Condition Specific SLs, Fig. 5C,D). Similarly, two published KRAS synthetic lethal genes, STK33 and YAP1, were only a dependency in minimal media conditions, but not in others providing a possible basis for why STK33 has been difficult to reproduce (Fig. 5D) (Babij et al., 2011; Luo et al., 2012; Scholl et al., 2009). Of the 26 literature synthetic lethal genes we analyzed, the vast majority (92%) demonstrated synthetic lethality only in specific media conditions or not at all in the conditions we tested. Although most of the synthetic lethal relationships were specific to certain conditions, some were independent of condition and were consistent synthetic lethal interactions the strongest and most consistent of which were BRCA1 and RGL1 (Fig. 5B,D). Together with our combinatorial genetic interaction map, these results demonstrate the dependence of most reported synthetic lethal genes on cellular and genetic context.

**KRAS mutant cells are DNA repair deficient and PARP inhibitor sensitive**

Our studies suggest that considering pathway, cellular and genetic context may help delineate robust synthetic lethal effects. We first developed a composite score based resiliency of a candidate SL gene based cellular and genetic context screens (Fig. 6A, see Methods). Ranking 31 single synthetic lethal

genes from our initial isogenic screen, we found that Network SL genes trended towards being more context independent than Literature SL genes (p=0.05 via rank sum test). This analysis identified the Network SL gene BRCA1 as a top candidate. Supporting this finding, our network meta-analysis identified two complexes involved in DNA repair and replication that included top hits from all three original RNAi studies including BRCA1 as well as POLR2G, POLR2D, POLR2B, RPA1, RPA2, RPA3 (Fig. 1D). Six out of seven genes in this network were also found in the top 5% of hits from three additional studies (Fig. 2). BRCA1 was the top hit in our single gene synthetic lethal screen, was a consistent synthetic lethal across media conditions (Fig. 5B), and had a lower than average number of genetic suppressors (Suppl Fig 3). Based on the function of BRCA1, we hypothesized that KRAS mutant cells harbor a unique dependence on DNA repair. We confirmed the dependency on BRCA1 in MCF10A-KRAS cells using independent siRNA reagents (Supplementary Fig. S4). We next sought further corroborative evidence of a DNA repair defect by identifying related chemically addressable vulnerabilities. An independent screen of 91 anti-cancer compounds highlighted several drugs targeting the DNA repair pathway as top hits in MCF10A KRAS G12D cells including WEE1, CHK1/2 and PARP inhibitors (Fig. 6B, Table 6). We validated PARP inhibitor sensitivity using three different PARP inhibitors, with talazoparib showing a ~1,000 fold difference in $IC_{50}$ between parental and KRAS mutant cells, and with rucaparib and olaparib demonstrating 2-5-fold sensitization (Fig. 6C, D). These PARP inhibitors equally inhibit PARP enzymatic activity, but talazoparib most strongly traps it onto DNA causing DNA double strand breaks that are preferentially repaired by homologous recombination via BRCA1 (Murai et al., 2012). Hence these KRAS cells have a dependence on BRCA1 that creates a vulnerability to PARP inhibition and are preferentially sensitive to agents that trap PARP onto chromatin.

We hypothesized that KRAS mutant cells are defective in DNA repair resulting in a dependency on this pathway to maintain genome fidelity. At baseline, KRAS-mutant cell lines harbored more γH2AX foci, a marker of DNA double strand breaks, compared to control cells indicating that mutant KRAS induces DNA damage (Fig. 6E, F). These results were independent of proliferation, as control and mutant cells grew at

the same rate (Fig. 3D). Treatment for 18 hours with talazoparib led to approximately equivalent amount of total DNA damage indicating that PARP inhibitors do not simply increase the induction double strand breaks in KRAS mutant cells (Fig. 6G). In contrast, after wash out of the PARP inhibitor, KRAS cells had a delay in the resolution of double strand breaks that persisted for at least 24 hours indicating that KRAS causes a deficiency in the repair of double strand breaks caused by PARP inhibition (Fig. 6G).

We sought to determine if sensitivity to PARP inhibitors was resilient against changes in cellular and genetic context, the same key features that led us to focus on BRCA1. Sensitivity to PARP inhibition in KRAS cells was independent of media conditions (Supplementary Fig. 5). Knockdowns of 191 genes against talazoparib treatment identified one suppressor, far lower than the number of suppressors associated with most of the genetic knockdowns in our study (Supplementary Fig. 3). Hence, PARP inhibition demonstrates KRAS synthetic lethality that is robust to changes both in genetic and cellular context in this system. To determine if these findings extended to other models of RAS mutant cancer we analyzed cells derived from skin tumors initiated in mice using a dimethylbenz[a]anthracene (DMBA)-initiated and a 12-O-tetradecanoylphorbol-13-acetate (TPA)-promoted two-stage skin carcinogenesis protocol resulting in tumors that characteristically harbor an oncogenic HRAS mutation (Balmain et al., 1984; Bonham et al., 1989). HRAS-mutant CCH85 carcinoma cells were sensitive to all three PARP inhibitors as compared to C5N keratinocytes controls with a 10-25 fold change in IC50 for talazoparib (Supplementary Fig. 6A) which was also corroborated in long term colony formation assays (Supplementary Fig. 6B). Next, we analyzed PARP inhibitor sensitivity in panels of cell lines derived from tumor types where RAS mutations are prevalent enough for statistical comparison in the genomics of drug sensitivity (GDSC) dataset which include colorectal, lung and ovarian cancer cell lines (Yang et al., 2013). Among these tumor types, we identified numerous significant associations between KRAS mutation and olaparib sensitivity ($p<0.002$ for Colorectal and ovarian, $p=3e-6$ overall, (Supplementary Fig. 6C). Compared to other mutations or copy number associations present in the genome, KRAS mutation was often among the top genomic features associated with olaparib sensitivity (Supplementary

Fig. 6D). We conclude that considering pathway, cellular and genetic context identifies a dependency on DNA repair that is targetable with PARP inhibitors warranting further investigation in other RAS-mutant cancers.

## DISCUSSION

The concept of synthetic lethality is an exciting approach to target cancer cells harboring specific cancer mutations that may otherwise be undruggable. We provide evidence for why most results from synthetic lethal studies have proven difficult to reproduce and offer a framework for identifying more robust synthetic lethal candidates. Recently improved genetic perturbation techniques such as those using CRISPR/Cas9 have led to renewed interest in synthetic lethal screening (Wang et al., 2016). We argue that these technologies alone cannot intrinsically overcome limitations due to differences in cellular and genetic context present between cancer models. We provide key experimental evidence for and strategies to resolve the differences in genetic context that have been thought to contribute to failures in synthetic lethal identification (Ashworth et al., 2011; Ryan et al., 2018).

Here we show that most synthetic lethals are highly dependent on cellular and genetic context. While testing published synthetic lethals we found that most were highly modified by cellular and genetic perturbations. For example, STK33 and GATA2 displayed synthetic lethality with KRAS only in a single isolated media condition and had among the most number of genetic suppressors. KRAS specific dependence on both these proteins has been disputed (Babij et al., 2011; Luo et al., 2012). We propose computational and experimental approaches that we anticipate will identify more robust synthetic lethal interactions for further study. First, we provide a computational approach that enables the identification of synthetic lethals that are more context independent. This retrospective approach leverages pathway information to integrate functional genomics data as opposed to previous work based on gene list analyses (Christodoulou et al., 2017; Downward, 2015). Second, we propose an experimental framework to rigorously test synthetic lethal effects using a panel of changes in cellular conditions as well as

screening against a panel of secondary perturbations to determine genetic resiliency, potentially using an E-MAP approach. In addition to changes in media conditions, variation may also be achieved by modulating the environment (e.g. hypoxia), growth density and batch of cell lines used (Ben-David et al., 2018). While our framework attempts to model the genetic and environmental heterogeneity present in cancers in a manner that is still amenable to high-throughput screening, future work could extend these approaches to vastly more secondary genetic perturbations as well as modulate the environment in different ways.

Applying our meta-analysis approach to three early KRAS screens we identified a set of networks representing protein pathways and complexes that were recurrently identified in different studies. Many components of these networks were found to re-validate in three held out studies and our isogenic model. Among these we investigated a network involved in DNA replication and repair. One component of this network, BRCA1, was a strong synthetic lethal regardless of cellular condition and had among the lowest number of genetic suppressors in our panel. The CCT complex, a chaperone complex involved in helping to fold part of the proteome (Yam et al., 2008), was also highlighted by our meta-analysis approach, and components of this complex were highlighted in 4 independent studies in total, warranting further investigation. This network framework enhances target discovery by accounting for pathway context in synthetic lethal screens in order to identify robust and potentially new targets for genetically defined cancers.

Our data highlight a potential role for PARP inhibitors in KRAS mutant cancers and warrants further investigation. PARP inhibitors inhibit PARP by both enzymatic inhibition as well as trapping PARP onto DNA and impairing replication during S-phase (Murai et al., 2012). We observed the most differential inhibition of wild-type versus KRAS mutant cells with the strongest PARP trapper, talazoparib suggesting that KRAS cells are dependent on unencumbered progression through S-phase which is consistent with the role of the DNA replication network we identified. This interaction was also evident in a chemically

induced murine tumor model and in small molecule profiling data across colorectal, lung and ovarian cancer cell lines tested for sensitivity to olaparib (Supplementary Fig 6). Both enhancement (Sun et al., 2017) and suppression (Gilad et al., 2010; Kalimutho et al., 2017; Kotsantis et al., 2016) of DNA repair processes have been linked with mutant KRAS. These differences may be explained by the cell line panel profiling results, where although KRAS mutant cells tend to be more sensitive to PARP inhibitors on average, a subset are more drug resistant. Therefore, one possibility is that additional genetic contexts not investigated in this study may influence this synthetic lethal relationship and determining which KRAS mutant contexts predict dependence on specific DNA repair pathways will require future work. In particular, such work may define the impact of changes in genetic context in terms of secondary mutations that co-occur with mutant KRAS, such as TP53 and LKB1, on PARP inhibitor sensitivity.

**ACKNOWLEDGMENTS**

The authors thank Alan Ashworth and Hayley Donnella for helpful discussions and assistance. This work was supported by National Cancer Institute grant nos. U01CA168370 (S.B.) and UC MEXUS Research grant DI-16-33 (A.A.K.)

**AUTHOR CONTRIBUTIONS**

Conceptualization, A.K. and S.B.; Methodology, A.K.; Software and formal Analysis, A.K., SB; Investigation: A.K., H.H., X.Z., S.K., W.D.; Resources, S.B., F.M., A.B; Supervision and Project Administration: S.B.; Writing: A.K., S.B.

**CONFLICT OF INTEREST STATEMENT**

S.B. consults with and/or receives research funding from Pfizer, Ideaya Biosciences and Revolution Medicines.

## METHODS

### Synthetic lethal screen analysis

We obtained screen data from supplementary information from the Luo, Steckel and Barbie studies and ranked all genes based on the scoring criterion reported in the supplementary material from each manuscript. Since the Barbie study only reported 250 hits as significant, this cutoff was used for further analysis and all other studies reported >250 hits. Significance in overlap between gene sets was determined by calculating a hypergometric p-value of overlap between the top 250 genes from each study, and setting the background tested genes. The hypergeometric was 1-phyper(x, m, n, k) (R Core Team, 2018) with x as the overlap in hits between study 1 and study 2, m is the number of total genes tested in study 1, n is the number of hits found in study 2 that were also tested in study 1, k is the top 250 hit genes in study 1.

For the human protein-protein interaction (PPI) dataset we downloaded all CORUM protein complexes and HumanNet PPIs with scores > 3 to derive a list of high confidence PPIs. In order to identify highly connected subnetworks we applied the MCODE clustering algorithm with default parameters to this network in Cytoscape and considered clusters with genes that were reported in multiple KRAS SL studies for downstream analysis (Bader and Hogue, 2003). Clusters were analyzed using the gProfiler web tool (Reimand et al., 2016) against the CORUM or the KEGG signaling pathway in order to functionally categorize clusters, with p-values of enrichment corrected for multiple testing. To determine the significance in network based overlap between two KRAS studies we randomly selected 250 genes from the list of genes tested in each study and determined the number of interactions spanning genes from two studies to establish a null distribution. This null distribution was compared to the actual overlap observed between two studies to determine a p-value defined as the fraction of 10,000 random simulations that had more interactions than what was observed in the real data.

To compare gene sets in additional studies we used a percentile approach because of the subjectivity evaluating a p-value cutoff to select hits from screening data of different types (i.e. isogenic vs cell line panels). To perform evaluation in held out KRAS SL screen datasets we obtained gene level screening data from three published KRAS studies (Costa-Cabral et al., 2016; Kim et al., 2013, 2016). Hits were taken as ranked in the Costa Cabral study. For the Kim studies genes were ranked into percentiles based on the average difference in essentiality scores between KRAS wild-type and mutant cell lines.

**Pathway Genetic Interaction Enrichment Analysis**

Genes were assigned to curated pathways based on a combination of the RAS 2.0 pathway annotations (https://www.cancer.gov/research/key-initiatives/ras/ras-central/blog/2015/ras-pathway-v2) and manual curation. The significance of sets of genetic interactions between a gene and a particular pathway was evaluated using a two-sided t-test to determine significance from a median of zero.

**Cell Lines & Tissue Culture**

MCF10A Isogenic cells were grown in three conditions for our experiments. Full Media defined as: DMEM/F12, 5% Horse Serum, 20ng/ml EGF, 0.5mg/ml Hydrocortisone, 100ng/ml Cholera Toxin, and 10ug/ml Insulin; Intermediate Media is DMEM/F12, 5% Horse Serum, 0.5mg/ml Hydrocortisone, 100ng/ml Cholera Toxin, and 10ug/ml Insulin; and Minimal Media is DMEM/F12 and 5% Horse Serum. Mouse cell lines were grown DMEM at 10%FBS plus 1X GlutaMAX (ThermoFisher #35050061).

**Western Blotting**

Cells were lysed with RIPA buffer (25mM Tri-HCl, ph 7.5, 150nM NaCl, 0.1% SDS, 1% Sodium deoxycholate, 10% Triton-X, 5mM EDTA, pH 8.0 for 30 minutes on ice and cell debris was pelleted and supernatant was collected and BCA protein quantification was used to obtain protein concentrations.

**RNAi Screening and Scoring**

1000 cells/well were reverse transfected in quadruplicate with 0.05µl/well of RNAiMax and 5ng/well of each esiRNA, 72 hours after transfection plates were fixed with 3% PFA, and permeabilized with 0.5% TritonX. Hoechst 33342 Solution (Themo #62249) was added at a final concentration of 4µg/mL and incubated at 37°C for 30 minutes. Nuclei were counted using a Thermo CellInsight microscope. Cell counts were normalized to a negative control non-targeting targeting esiRNA included in each plate and a Student's t-test was used to determine a p-value of significance by comparing normalized counts for each esiRNA in KRAS versus eGFP cells. Genetic interactions scores were based on $Log_{10}$(p-value) and signed to reflect synthetic sickness (negative) and enhancement (positive). P-values were used to estimate false discovery rates (FDR) using Benjamin-Hochberg method (Benjamini and Hochberg, 1995). For esiRNA studies non-targeting esiRNA targeting eGFP (Sigma, #EHUEGFP). For siRNA studies, siBRCA1 is an ON-TARGET SMARTpool (Dharmacon, #L-003461-00-0005) and siNT is ON-TARGET NT4 (Dharmacon #D001810-04-05).

For the combinatorial E-MAP screen 5ng of each of 96 esiRNAs ("array") was plated in quadruplicate into 384 well plates to which was added a second constant "query" esiRNA (5ng) using a Mantis Liquid Handler to all wells along with 10 µl of RNAiMax to prepare reverse transfection mix, cells were plated and allowed to grow for 72 hours. At end point plates were processed as above for cell count. Counts were normalized to the median of each plate and Z-scored. Four replicates were averaged to obtain a mean Z-score per esiRNA combination.

The cellular context score of each gene was defined as the variance of KRAS genetic interaction scores across three conditions. The genetic context score was based on the number of significant genetic suppressors (E-MAP interaction score $Z>2$) identified for each gene. The product of these two metrics was used to define the ranking and then Z-normalized for visualization.

**Drug Screening**

1000 cells/well in a 384 well plate were seeded and exposed to the drug library the next day. Drug plates were prepared by diluting stock drug into a 4 replicate 4-point dilutions series (500, 250, 50, 5ng/mL). Each dose was added in 4 replicates using a Caliper Zephyr liquid handler. Cells were allowed to grow for 72 hours before nuclei counting. Cell counts were normalized to DMSO control wells and area under the dose-response curve (AUC) was calculated as the sum of proliferation values over all 4 concentrations.

**γH2AX Immunofluorescence**

Cells were plated into 6-well plates containing coverslips and allowed to grow overnight prior to treatment with talazoparib. For washout, cells were washed twice with PBS, and allowed to grow in fresh media without talazoparib. Cells were fixed using 4% PFA for 10 minutes at room temperature, permeabilized using 0.3% Triton-X in DPBS, and blocked with 3% BSA in PBS. Cells were incubated with the primary antibody overnight at 4 C (Anti-Histone γ-H2AX, #07-627 clone PC130, Millipore Sigma 1:1000) and the secondary antibody (Goat anti-Mouse Alexa Fluor 647 Polyclonal, Thermo Fisher) for 1 hour at room temperature. Following washes with PBS and water, coverslips were mounted using Prolong Antifade containing DAPI (P36931). Foci were quantified using ImageJ plugin Foci Counter (The Bioimaging Center, University of Konstanz).

**Drug response curves and colony formation assays**

For IC50 determination, 500 cells were seeded into 384-well plates overnight, then exposed to drugs and allowed to proliferate for 96 hours. Cells were quantified using nuclei counting and compared to cell counts with DMSO treatment. Curves were fit and IC50 determined using Graphad Prism nonlinear regression analysis. For colony formation assays, 500 cells were plated onto 12-well plates overnight before drug addition. Media and drugs were changed every 72 hours. Cells were fixed and stained with 1% crystal violet in 20% methanol. Plates were washed with water, dried and imaged using Epson V600 scanner.

**REFERENCES**


Ashworth, A., and Lord, C.J. (2018). Synthetic lethal therapies for cancer: what's next after PARP inhibitors? Nat. Rev. Clin. Oncol. 1.

Ashworth, A., Lord, C.J., and Reis-Filho, J.S. (2011). Genetic Interactions in Cancer Progression and Treatment. Cell *145*, 30–38.

Babij, C., Zhang, Y., Kurzeja, R.J., Munzli, A., Shehabeldin, A., Fernando, M., Quon, K., Kassner, P.D., Ruefli-Brasse, A.A., Watson, V.J., et al. (2011). STK33 kinase activity is nonessential in KRAS-dependent cancer cells. Cancer Res. *71*, 5818–5826.

Bader, G.D., and Hogue, C.W. (2003). An automated method for finding molecular complexes in large protein interaction networks. BMC Bioinformatics *4*, 2.

Balmain, A., Ramsden, M., Bowden, G.T., and Smith, J. (1984). Activation of the mouse cellular Harvey-ras gene in chemically induced benign skin papillomas. Nature *307*, 658–660.

Bandyopadhyay, S., Mehta, M., Kuo, D., Sung, M.-K., Chuang, R., Jaehnig, E.J., Bodenmiller, B., Licon, K., Copeland, W., Shales, M., et al. (2010). Rewiring of Genetic Networks in Response to DNA Damage. Science *330*, 1385–1389.

Barbie, D.A., Tamayo, P., Boehm, J.S., Kim, S.Y., Moody, S.E., Dunn, I.F., Schinzel, A.C., Sandy, P., Meylan, E., Scholl, C., et al. (2009). Systematic RNA interference reveals that oncogenic KRAS-driven cancers require TBK1. Nature *462*, 108–112.

Ben-David, U., Siranosian, B., Ha, G., Tang, H., Oren, Y., Hinohara, K., Strathdee, C.A., Dempster, J., Lyons, N.J., Burns, R., et al. (2018). Genetic and transcriptional evolution alters cancer cell line drug response. Nature *560*, 325–330.

Benjamini, Y., and Hochberg, Y. (1995). Controlling the False Discovery Rate: A Practical and Powerful Approach to Multiple Testing. J. R. Stat. Soc. Ser. B Methodol. *57*, 289–300.

Bonham, K., Embry, T., Gibson, D., Jaffe, D.R., Roberts, R.A., Cress, A.E., and Bowden, G.T. (1989). Activation of the cellular Harvey ras gene in mouse skin tumors initiated with urethane. Mol. Carcinog. *2*, 34–39.

Boone, C., Bussey, H., and Andrews, B.J. (2007). Exploring genetic interactions and networks with yeast. Nat. Rev. Genet. *8*, 437–449.

Bryant, H.E., Schultz, N., Thomas, H.D., Parker, K.M., Flower, D., Lopez, E., Kyle, S., Meuth, M., Curtin, N.J., and Helleday, T. (2005). Specific killing of BRCA2-deficient tumours with inhibitors of poly(ADP-ribose) polymerase. Nature *434*, 913–917.

Christodoulou, E.G., Yang, H., Lademann, F., Pilarsky, C., Beyer, A., and Schroeder, M. (2017). Detection of COPB2 as a KRAS synthetic lethal partner through integration of functional genomics screens. Oncotarget *8*, 34283–34297.

Collins, S.R., Miller, K.M., Maas, N.L., Roguev, A., Fillingham, J., Chu, C.S., Schuldiner, M., Gebbia, M., Recht, J., Shales, M., et al. (2007). Functional dissection of protein complexes involved in yeast chromosome biology using a genetic interaction map. Nature *446*, 806–810.

Costa-Cabral, S., Brough, R., Konde, A., Aarts, M., Campbell, J., Marinari, E., Riffell, J., Bardelli, A., Torrance, C., Lord, C.J., et al. (2016). CDK1 Is a Synthetic Lethal Target for KRAS Mutant Tumours. PloS One *11*, e0149099.

Costanzo, M., Baryshnikova, A., Bellay, J., Kim, Y., Spear, E.D., Sevier, C.S., Ding, H., Koh, J.L.Y., Toufighi, K., Mostafavi, S., et al. (2010). The genetic landscape of a cell. Science *327*, 425–431.

Costanzo, M., VanderSluis, B., Koch, E.N., Baryshnikova, A., Pons, C., Tan, G., Wang, W., Usaj, M., Hanchard, J., Lee, S.D., et al. (2016). A global genetic interaction network maps a wiring diagram of cellular function. Science *353*.

Ding, L., Getz, G., Wheeler, D.A., Mardis, E.R., McLellan, M.D., Cibulskis, K., Sougnez, C., Greulich, H., Muzny, D.M., Morgan, M.B., et al. (2008). Somatic mutations affect key pathways in lung adenocarcinoma. Nature *455*, 1069–1075.

Downward, J. (2015). RAS Synthetic Lethal Screens Revisited: Still Seeking the Elusive Prize? Clin. Cancer Res. *21*, 1802–1809.

Farmer, H., McCabe, N., Lord, C.J., Tutt, A.N.J., Johnson, D.A., Richardson, T.B., Santarosa, M., Dillon, K.J., Hickson, I., Knights, C., et al. (2005). Targeting the DNA repair defect in *BRCA* mutant cells as a therapeutic strategy. Nature *434*, 917–921.

Fröhling, S., and Scholl, C. (2011). STK33 Kinase Is Not Essential in KRAS-Dependent Cells–Letter. Cancer Res. *71*, 7716–7716.

Galardini, M., Busby, B.P., Vieitez, C., Dunham, A.S., Typas, A., and Beltrao, P. (2018). The impact of the genetic background on gene deletion phenotypes in Saccharomyces cerevisiae. BioRxiv 487439.

Gilad, O., Nabet, B.Y., Ragland, R.L., Schoppy, D.W., Smith, K.D., Durham, A.C., and Brown, E.J. (2010). Combining ATR suppression with oncogenic Ras synergistically increases genomic instability, causing synthetic lethality or tumorigenesis in a dosage-dependent manner. Cancer Res. *70*, 9693–9702.

Guarente, L. (1993). Synthetic enhancement in gene interaction: a genetic tool come of age. Trends Genet. TIG *9*, 362–366.

Kalimutho, M., Bain, A.L., Mukherjee, B., Nag, P., Nanayakkara, D.M., Harten, S.K., Harris, J.L., Subramanian, G.N., Sinha, D., Shirasawa, S., et al. (2017). Enhanced dependency of KRAS-mutant colorectal cancer cells on RAD51-dependent homologous recombination repair identified from genetic interactions in Saccharomyces cerevisiae. Mol. Oncol. *11*, 470–490.

Kim, H.S., Mendiratta, S., Kim, J., Pecot, C.V., Larsen, J.E., Zubovych, I., Seo, B.Y., Kim, J., Eskiocak, B., Chung, H., et al. (2013). Systematic Identification of Molecular Subtype-Selective Vulnerabilities in Non Small Cell Lung Cancer. Cell *155*.

Kim, J., McMillan, E., Kim, H.S., Venkateswaran, N., Makkar, G., Rodriguez-Canales, J., Villalobos, P., Neggers, J.E., Mendiratta, S., Wei, S., et al. (2016). XPO1-dependent nuclear export is a druggable vulnerability in KRAS-mutant lung cancer. Nature *advance online publication*.

Kotsantis, P., Silva, L.M., Irmscher, S., Jones, R.M., Folkes, L., Gromak, N., and Petermann, E. (2016). Increased global transcription activity as a mechanism of replication stress in cancer. Nat. Commun. *7*, 13087.

Lee, I., Blom, U.M., Wang, P.I., Shim, J.E., and Marcotte, E.M. (2011). Prioritizing candidate disease genes by network-based boosting of genome-wide association data. Genome Res. *21*, 1109–1121.

Lord, C.J., and Ashworth, A. (2016). BRCAness revisited. Nat. Rev. Cancer *16*, 110–120.

Luo, J., Emanuele, M.J., Li, D., Creighton, C.J., Schlabach, M.R., Westbrook, T.F., Wong, K.-K., and Elledge, S.J. (2009). A Genome-wide RNAi Screen Identifies Multiple Synthetic Lethal Interactions with the Ras Oncogene. Cell *137*, 835–848.

Luo, T., Masson, K., Jaffe, J.D., Silkworth, W., Ross, N.T., Scherer, C.A., Scholl, C., Fröhling, S., Carr, S.A., Stern, A.M., et al. (2012). STK33 kinase inhibitor BRD-8899 has no effect on KRAS-dependent cancer cell viability. Proc. Natl. Acad. Sci. U. S. A. *109*, 2860–2865.

Martins, M.M., Zhou, A.Y., Corella, A., Horiuchi, D., Yau, C., Rakshandehroo, T., Gordan, J.D., Levin, R.S., Johnson, J., Jascur, J., et al. (2015). Linking Tumor Mutations to Drug Responses via a Quantitative Chemical–Genetic Interaction Map. Cancer Discov. *5*, 154–167.

McGillicuddy, N., Floris, P., Albrecht, S., and Bones, J. (2018). Examining the sources of variability in cell culture media used for biopharmaceutical production. Biotechnol. Lett. *40*, 5–21.

Modrek, B., Ge, L., Pandita, A., Lin, E., Mohan, S., Yue, P., Guerrero, S., Lin, W.M., Pham, T., Modrusan, Z., et al. (2009). Oncogenic activating mutations are associated with local copy gain. Mol. Cancer Res. MCR *7*, 1244–1252.

Mullard, A. (2017). Synthetic lethality screens point the way to new cancer drug targets. Nat. Rev. Drug Discov. *16*, 736.

Murai, J., Huang, S.N., Das, B.B., Renaud, A., Zhang, Y., Doroshow, J.H., Ji, J., Takeda, S., and Pommier, Y. (2012). Trapping of PARP1 and PARP2 by Clinical PARP Inhibitors. Cancer Res. *72*, 5588–5599.

R Core Team (2018). R: The Hypergeometric Distribution.

Rancati, G., Moffat, J., Typas, A., and Pavelka, N. (2018). Emerging and evolving concepts in gene essentiality. Nat. Rev. Genet. *19*, 34–49.

Reimand, J., Arak, T., Adler, P., Kolberg, L., Reisberg, S., Peterson, H., and Vilo, J. (2016). g:Profiler-a web server for functional interpretation of gene lists (2016 update). Nucleic Acids Res. *44*, W83-89.

Roguev, A., Talbot, D., Negri, G.L., Shales, M., Cagney, G., Bandyopadhyay, S., Panning, B., and Krogan, N.J. (2013). Quantitative genetic-interaction mapping in mammalian cells. Nat. Methods *10*, 432–437.

Ruepp, A., Waegele, B., Lechner, M., Brauner, B., Dunger-Kaltenbach, I., Fobo, G., Frishman, G., Montrone, C., and Mewes, H.-W. (2010). CORUM: the comprehensive resource of mammalian protein complexes—2009. Nucleic Acids Res. *38*, D497–D501.

Ryan, C.J., Bajrami, I., and Lord, C.J. (2018). Synthetic Lethality and Cancer - Penetrance as the Major Barrier. Trends Cancer *4*, 671–683.

Scholl, C., Fröhling, S., Dunn, I.F., Schinzel, A.C., Barbie, D.A., Kim, S.Y., Silver, S.J., Tamayo, P., Wadlow, R.C., Ramaswamy, S., et al. (2009). Synthetic Lethal Interaction between Oncogenic KRAS Dependency and STK33 Suppression in Human Cancer Cells. Cell *137*, 821–834.

Settleman, J., Sawyers, C.L., and Hunter, T. (2018). Challenges in validating candidate therapeutic targets in cancer. ELife *7*, e32402.

Steckel, M., Molina-Arcas, M., Weigelt, B., Marani, M., Warne, P.H., Kuznetsov, H., Kelly, G., Saunders, B., Howell, M., Downward, J., et al. (2012). Determination of synthetic lethal interactions in KRAS oncogene-dependent cancer cells reveals novel therapeutic targeting strategies. Cell Res. *22*, 1227–1245.

Stein, A. (2007). Decreasing variability in your cell culture. BioTechniques *43*, 228–229.

Stolze, B., Reinhart, S., Bulllinger, L., Fröhling, S., and Scholl, C. (2015). Comparative analysis of KRAS codon 12, 13, 18, 61, and 117 mutations using human MCF10A isogenic cell lines. Sci. Rep. *5*, 8535.

Sun, C., Fang, Y., Yin, J., Chen, J., Ju, Z., Zhang, D., Chen, X., Vellano, C.P., Jeong, K.J., Ng, P.K.-S., et al. (2017). Rational combination therapy with PARP and MEK inhibitors capitalizes on therapeutic liabilities in RAS mutant cancers. Sci. Transl. Med. *9*.

Tessema, M., Yingling, C.M., Snider, A.M., Do, K., Juri, D.E., Picchi, M.A., Zhang, X., Liu, Y., Leng, S., Tellez, C.S., et al. (2014). GATA2 is epigenetically repressed in human and mouse lung tumors and is not requisite for survival of KRAS mutant lung cancer. J. Thorac. Oncol. Off. Publ. Int. Assoc. Study Lung Cancer *9*, 784–793.

Wang, H., La Russa, M., and Qi, L.S. (2016). CRISPR/Cas9 in Genome Editing and Beyond. Annu. Rev. Biochem. *85*, 227–264.

Yam, A.Y., Xia, Y., Lin, H.-T.J., Burlingame, A., Gerstein, M., and Frydman, J. (2008). Defining the TRiC/CCT interactome links chaperonin function to stabilization of newly made proteins with complex topologies. Nat. Struct. Mol. Biol. *15*, 1255–1262.

Yang, W., Soares, J., Greninger, P., Edelman, E.J., Lightfoot, H., Forbes, S., Bindal, N., Beare, D., Smith, J.A., Thompson, I.R., et al. (2013). Genomics of Drug Sensitivity in Cancer (GDSC): a resource for therapeutic biomarker discovery in cancer cells. Nucleic Acids Res. *41*, D955-961.

**SUPPLEMENTARY TABLES**

Table 1: Gene lists used for network analysis

Table 2: List of genes in KRAS synthetic lethal networks, their source and association with protein complexes or pathways and list of KRAS synthetic lethals and their source

Table 3: esiRNA library genes and annotations

Table 4: Single gene scores the KRAS synthetic lethal screens and media condition screens in isogenic cells

Table 5: E-MAP scores for gene pairs in KRAS G12D cells.

Table 6: Scores for drug screen in KRAS mutant versus control eGFP cell lines.

**FIGURE LEGENDS**

**Figure 1. Meta-analysis of published studies identifies common KRAS synthetic lethal networks.** (A) Gene overlap between the top 250 hit genes reported from three published KRAS synthetic lethal studies, Luo et al, Barbie et al., and Steckel et al. (Barbie et al., 2009; Luo et al., 2009; Steckel et al., 2012). P-values based on two-tailed hypergeometric test calculated between pairwise comparisons taking into account all tested genes per study. (B) Data integration strategy for mapping top 250 KRAS synthetic lethal reported from each study onto a protein-protein interaction network composed on interactions from HumanNet and CORUM protein complexes. The number of genes that were tested in each study, n. (C) Comparison of the number of interactions observed in the protein-protein interaction (PPI) network spanning between hits reported in the two indicated studies versus the number of similar interactions observed between random genes. Histogram represents results from 10,000 simulations conducted from randomly picking 250 genes that were tested in each respective study and the p-value represents the fraction of simulations where the same or more interactions than the actual observed number were obtained. (D) The PPI network was limited to interactions where at least one of the proteins was identified in previous studies and then subjected to network clustering to identify densely connected components using MCODE. Individual subnetworks were filtered to those which contained genes from multiple studies and grouped based on gene function into 7 clusters. The set of genes identified in each subnetwork was assessed for overlap with the CORUM or KEGG complex or pathway listed using a two-tailed hypergeometric test.

**Figure 2. Comparison of genes in KRAS synthetic lethal networks and previously published KRAS synthetic lethal genes in held-out studies.** 105 predicted KRAS synthetic lethal network genes and 26 previously published KRAS synthetic lethals were evaluated using data from Kim et al 2013, Kim et al 2016, and Costa-Cabral et al. (Costa-Cabral et al., 2016; Kim et al., 2013, 2016). Genes in each study were ranked into percentiles based on the difference in proliferation after knockdown in KRAS-mutant versus wild-type cell lines. The lower the percentile the more evidence for KRAS specific synthetic lethality.

Accuracy calculated as the number of genes in the top 5% (pink dots) out of all the tested genes per category. The number of genes tested in each study, n.

**Figure 3. A new isogenic cell line screen validates KRAS synthetic lethal network genes.** (A) Overview of approach. MCF10A cells stably expressing eGFP or a mutant KRAS construct were reverse transfected with esiRNAs targeting specific genes. After 72 hours, relative proliferation was compared between eGFP and KRAS mutant cells to score genetic interactions. (B) Proliferation based on cell count of uniformly plated MCF10A cells expressing eGFP, KRAS G12V or G12D grown in the presence or absence of 20ng/ml EGF for 72 hours. (C) Immunoblot of lysates from isogenic cells grown in the presence or absence of 20ng/ml EGF for 24 hours. (D) Proliferation of eGFP or KRAS G12D cells grown in the indicated media conditions after non-targeting (NT) or KRAS knockdown for 72 hours, normalized to NT control. (E) Volcano plot of KRAS G12D screen reflecting the magnitude of change in proliferation after gene knockdown in KRAS G12D versus eGFP expressing lines versus the significance of this effect calculated among replicates. Dotted lines represent the indicated false discovery rate (FDR) cutoffs. (F) Relative proliferation of knockdown of listed genes in eGFP or KRAS G12D cells compared to non-targeting control in each respective cell line. Genes selected based on genetic interactions with <1% FDR. (G) Signed genetic interaction scores for genes in the broader RAS pathway grouped into functional categories. The most negative scoring genes in each category are listed. (H) Signed genetic interaction score of retested literature curated KRAS synthetic lethal genes and their source. Only a subset of genes from Luo et al. are indicated for clarity. (I) Comparison of genetic interaction scores for genes involved in the RAS or MAPK pathway (RAS/MAPK), RTK signaling, KRAS synthetic lethal genes from the literature (green), or predicted synthetic lethal network genes (purple). P-values based on comparison against a median interaction score of zero (bottom) and between groups (above), both by two-tailed Student's t-test. Boxes represent the median, hinges span 25-75$^{th}$ percentile and whiskers span 10-90$^{th}$ percentile. Error bars are s.d.

**Figure 4. A genetic interaction map identifies KRAS synthetic lethal suppressors.** (A) Overview of approach to generate an epistatic mini-array profile (E-MAP) using combinatorial RNAi to measure 5,828 pairwise genetic interactions in MCF10A KRAS G12D cells. esiRNAs targeting a set of genes are arrayed in a pairwise fashion (in quadruplicate) in tissue culture plates. Reverse transfection is then performed, and the resulting fitness defects are observed using high-content imaging. Raw data is normalized and scored (see Methods) (B) Overview of genetic interaction map for 30 KRAS synthetic lethal genes and candidate modifiers. Interactions scoring >2 or <-2 are shown. (C) Relative proliferation of knockdown of three KRAS synthetic lethals identified or confirmed in this study, CCND1, CDK6 and STK33, in eGFP or KRAS G12D MCF10A cells alone and in combination with their top positive interaction partners. Proliferation normalized to mock. P-values based on a two-sided t-test, error bars s.d. (D) Categorical annotations for groups of genes displaying significantly strong genetic interactions with synthetic lethal query genes with $p<0.01$ (see Methods). (E) Genetic interaction partners involving two KRAS synthetic lethal genes identified in this study, RGL1 and DNMT3A, and associated pathways enriched for genetic interactions. Edge thickness is proportional to interaction score.

**Figure 5. Dependency on synthetic lethal genes vary based on cellular conditions.** (A) Knockdown of KRAS or non-targeting (NT) in MCF10A eGFP or KRAS G12D cells in the indicated media condition for 72 hours. Proliferation measured relative to NT. (B) Heatmap of genetic interaction scores for KRAS G12D cells grown in full, intermediate or minimal media conditions compared to eGFP cells. Highlighted gene sets show consistent or condition specific synthetic lethality across conditions. Red arrow highlights BRCA1 as a consistent KRAS synthetic lethal. (C) Heatmap of genetic interaction scores for previously published KRAS synthetic lethals across different growth conditions. (D) Proliferation of cells grown in the indicated conditions harboring knockdown of indicated genes normalized to NT transfection control. Full = full media, Int = intermediate media, Min = minimal media. Error bars are s.d.

**Figure 6. PARP inhibitors are more effective in oncogenic KRAS expressing cells.** (A) Ranking of candidate KRAS synthetic lethal genes based on integration of genetic and cellular perturbation screens. Genes were selected for analysis based on evidence of synthetic lethality in MCF10A KRAS cells grown in minimal media. The conceptual source of each gene is listed. (B) Drug screen of 91 clinically relevant compounds ranked by sensitivity based on difference in the drug area under the curve (AUC) between eGFP and KRAS G12D cells. DMSO and EGFR inhibitors indicated as controls for no effect and KRAS induced drug resistance, respectively. (C) Relative proliferation of control eGFP, KRAS G12D or G12V expressing MCF10A lines after treatment with PARP inhibitors talazoparib, rucaparib or olaparib for 72 hours. $IC_{50}$ values are shown. (D) Long-term clonogenic growth of MCF10A KRAS G12D and eGFP cells treated with DMSO or talazoparib for two weeks. (E) γH2AX immunofluorescence in eGFP or G12D expressing cells, red. Nuclei outlines in dotted lines based on DAPI staining. (F) Quantification of $\gamma$ H2AX foci in the indicated cell lines treated with DMSO or with 500nM of talazoparib for 18 hours. (G) Treatment of the indicated cells with 500nM talazoparib for 18 hours then washed out. γH2AX foci quantified before, 8 and 24 hours after washout. Error bars, s.d. except E and F which are s.e.m. Not significant, n.s.

# FIGURES

## Figure 1

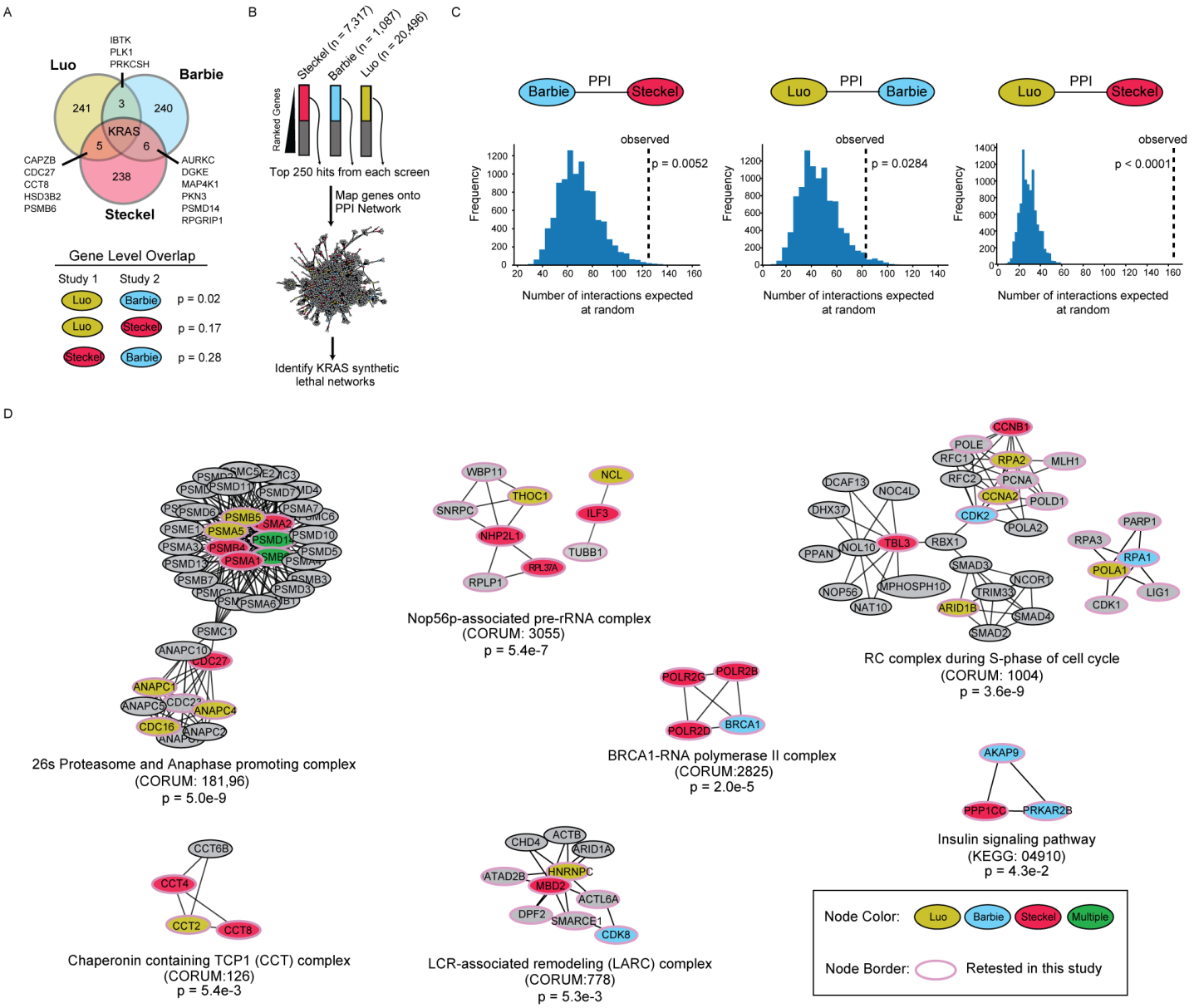

**Figure 2**

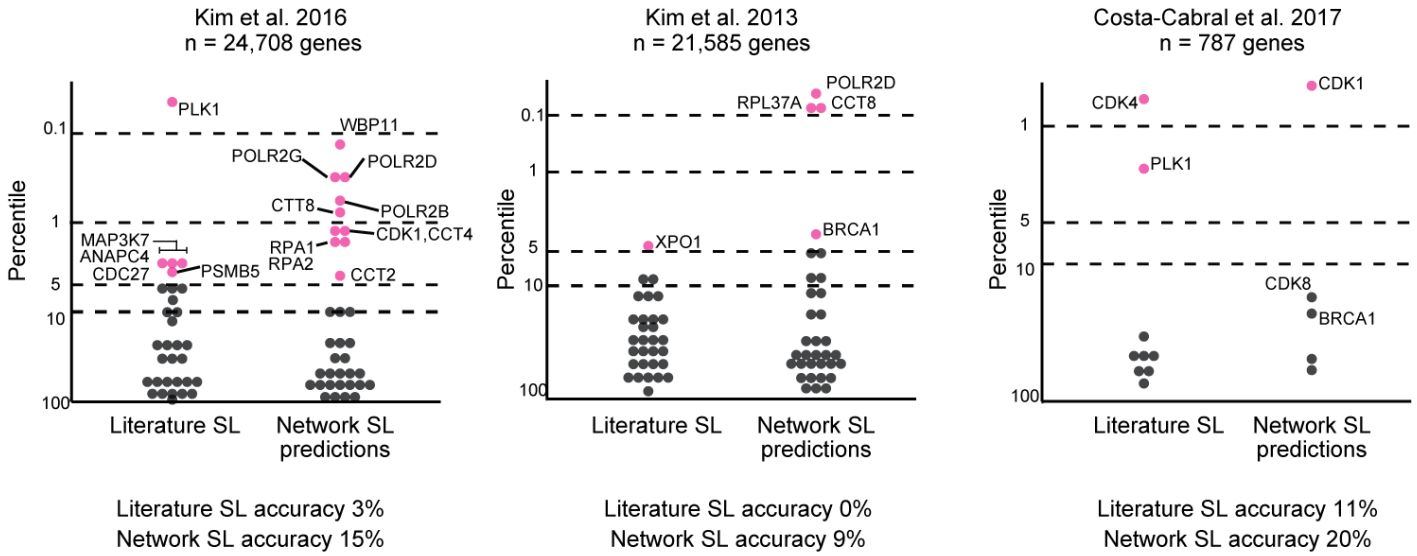
Kim et al. 2016
n = 24,708 genes
Percentile
0.1
1
5
10
100
PLK1
WBP11
POLR2G
POLR2D
CTT8
POLR2B
CDK1,CCT4
MAP3K7
ANAPC4
CDC27
PSMB5
RPA1
RPA2
CCT2
Literature SL
Network SL predictions
Literature SL accuracy 3%
Network SL accuracy 15%
Kim et al. 2013
n = 21,585 genes
Percentile
0.1
1
5
10
100
POLR2D
RPL37A
CCT8
XPO1
BRCA1
Literature SL
Network SL predictions
Literature SL accuracy 0%
Network SL accuracy 9%
Costa-Cabral et al. 2017
n = 787 genes
Percentile
1
5
10
100
CDK1
CDK4
PLK1
CDK8
BRCA1
Literature SL
Network SL predictions
Literature SL accuracy 11%
Network SL accuracy 20%

# Figure 3

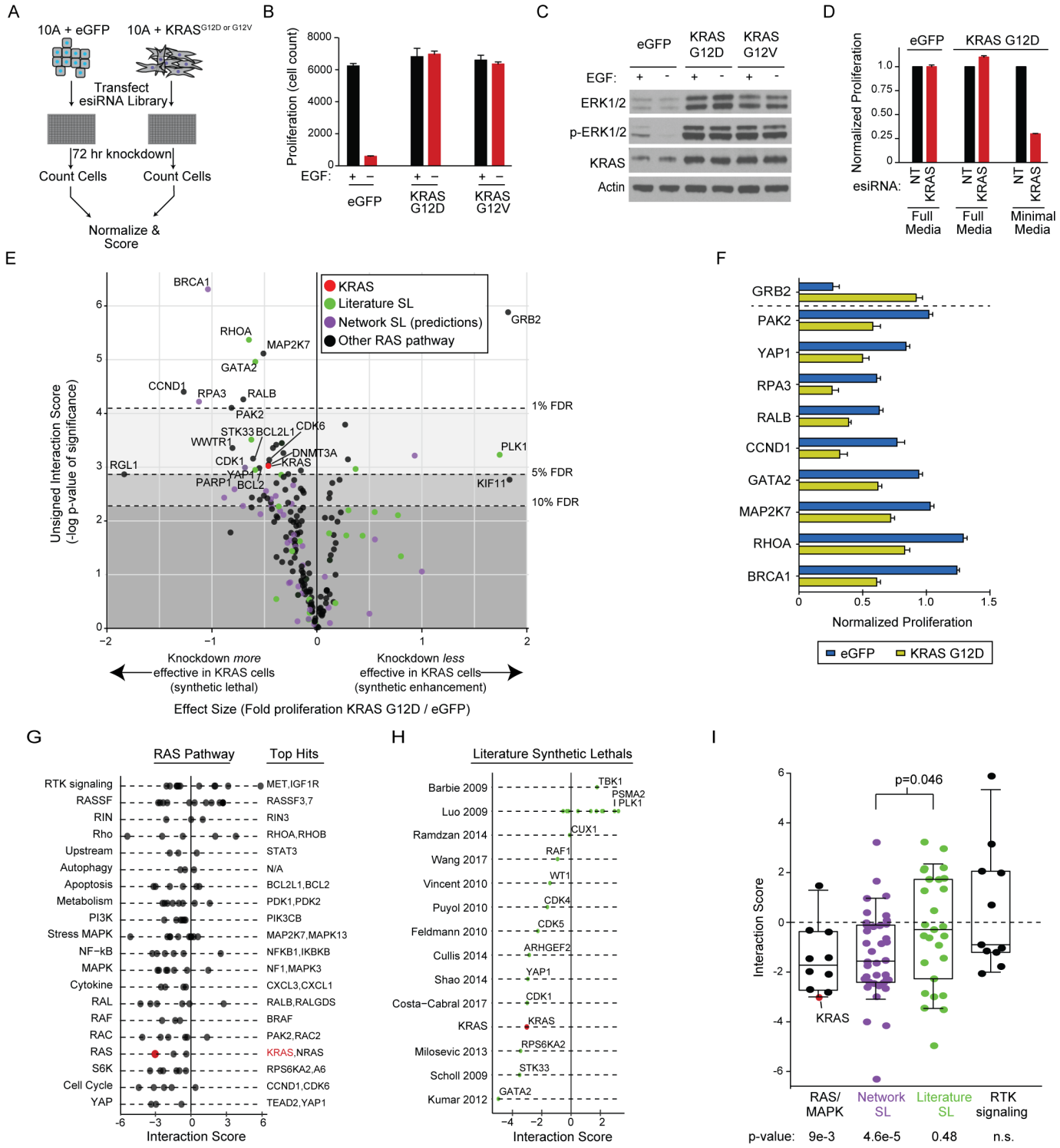
A
10A + eGFP
10A + KRAS G12D or G12V
Transfect esiRNA Library
72 hr knockdown
Count Cells
Count Cells
Normalize & Score
B
Proliferation (cell count)
EGF:
eGFP
KRAS G12D
KRAS G12V
C
eGFP
KRAS G12D
KRAS G12V
EGF:
ERK1/2
p-ERK1/2
KRAS
Actin
D
eGFP
KRAS G12D
Normalized Proliferation
esiRNA:
NT
KRAS
Full Media
Minimal Media
E
KRAS
Literature SL
Network SL (predictions)
Other RAS pathway
1% FDR
5% FDR
10% FDR
Unsigned Interaction Score (-log p-value of significance)
Knockdown more effective in KRAS cells (synthetic lethal)
Knockdown less effective in KRAS cells (synthetic enhancement)
Effect Size (Fold proliferation KRAS G12D / eGFP)
F
Normalized Proliferation
eGFP
KRAS G12D
G
RAS Pathway
Top Hits
Interaction Score
H
Literature Synthetic Lethals
Interaction Score
I
p=0.046
Interaction Score
RAS/ MAPK
Network SL
Literature SL
RTK signaling
p-value:
9e-3
4.6e-5
0.48
n.s.

# Figure 4

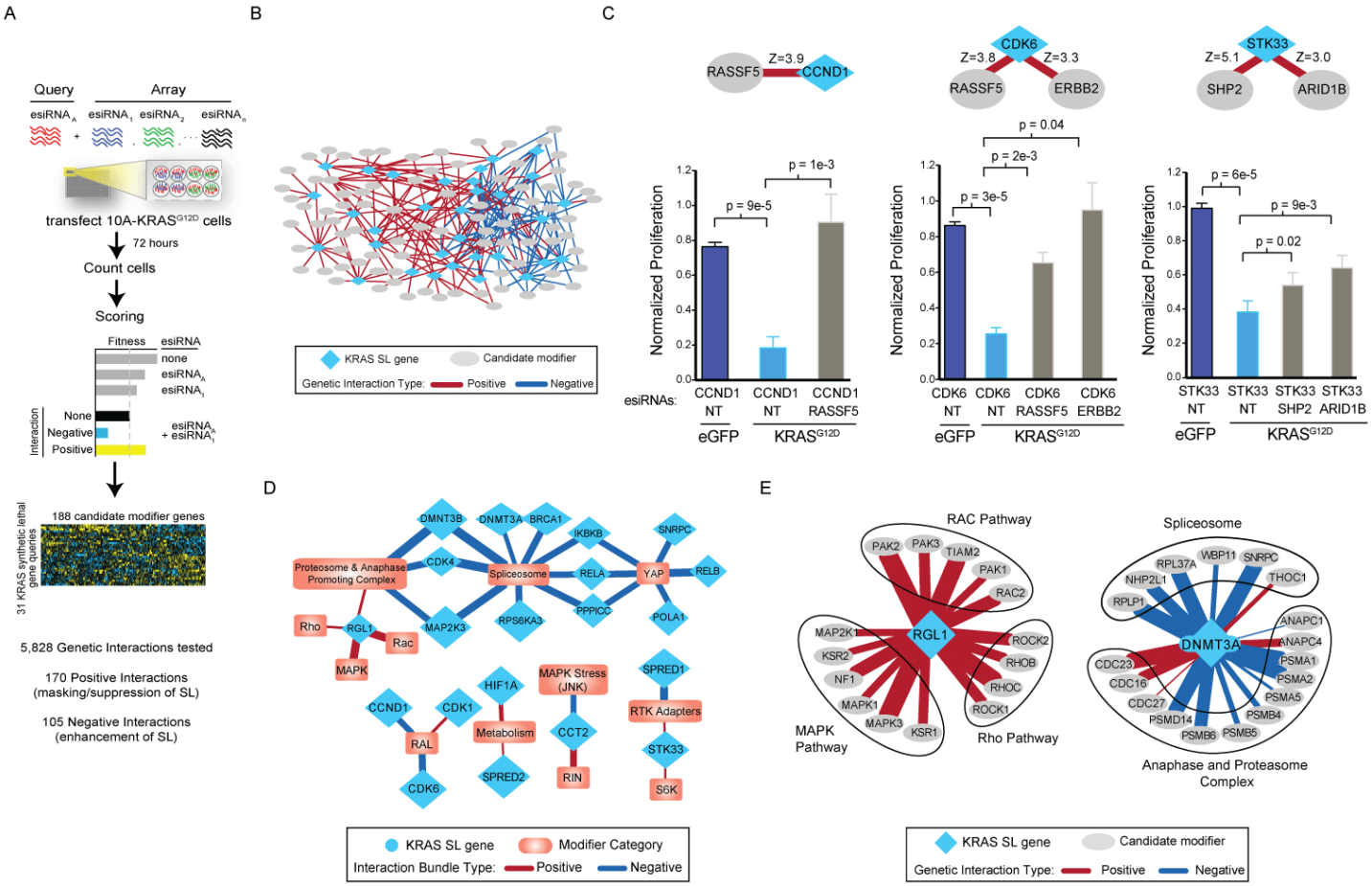
A
Query
Array
esiRNA_A
esiRNA_1
esiRNA_2
esiRNA_n
transfect 10A-KRAS^G12D cells
72 hours
Count cells
Scoring
Fitness
esiRNA
none
esiRNA_A
esiRNA_1
Interaction
None
Negative
Positive
esiRNA_A + esiRNA_1
188 candidate modifier genes
31 KRAS synthetic lethal gene queries
5,828 Genetic Interactions tested
170 Positive Interactions (masking/suppression of SL)
105 Negative Interactions (enhancement of SL)
B
KRAS SL gene
Candidate modifier
Genetic Interaction Type:
Positive
Negative
C
RASSF5
Z=3.9
CCND1
CDK6
Z=3.8
Z=3.3
RASSF5
ERBB2
STK33
Z=5.1
Z=3.0
SHP2
ARID1B
Normalized Proliferation
p = 9e-5
p = 1e-3
p = 3e-5
p = 2e-3
p = 0.04
p = 6e-5
p = 9e-3
p = 0.02
esiRNAs:
CCND1 NT
CCND1 NT
CCND1 RASSF5
CDK6 NT
CDK6 NT
CDK6 RASSF5
CDK6 ERBB2
STK33 NT
STK33 NT
STK33 SHP2
STK33 ARID1B
eGFP
KRAS^G12D
D
DMNT3B
DNMT3A
BRCA1
IKBKB
SNRPC
Proteosome & Anaphase Promoting Complex
CDK4
Spliceosome
RELA
YAP
RELB
Rho
RGL1
Rac
MAP2K3
RPS6KA3
PPPICC
POLA1
MAPK
CCND1
CDK1
HIF1A
MAPK Stress (JNK)
SPRED1
RAL
Metabolism
CCT2
RTK Adapters
CDK6
SPRED2
RIN
STK33
S6K
KRAS SL gene
Modifier Category
Interaction Bundle Type:
Positive
Negative
E
RAC Pathway
PAK2
PAK3
TIAM2
PAK1
RAC2
MAP2K1
RGL1
ROCK2
KSR2
RHOB
NF1
RHOC
MAPK1
ROCK1
MAPK3
KSR1
MAPK Pathway
Rho Pathway
Spliceosome
WBP11
SNRPC
RPL37A
NHP2L1
THOC1
RPLP1
ANAPC1
DNMT3A
ANAPC4
PSMA1
CDC23
PSMA2
CDC16
PSMA5
CDC27
PSMB4
PSMD14
PSMB6
PSMB5
Anaphase and Proteasome Complex
KRAS SL gene
Candidate modifier
Genetic Interaction Type:
Positive
Negative

# Figure 5

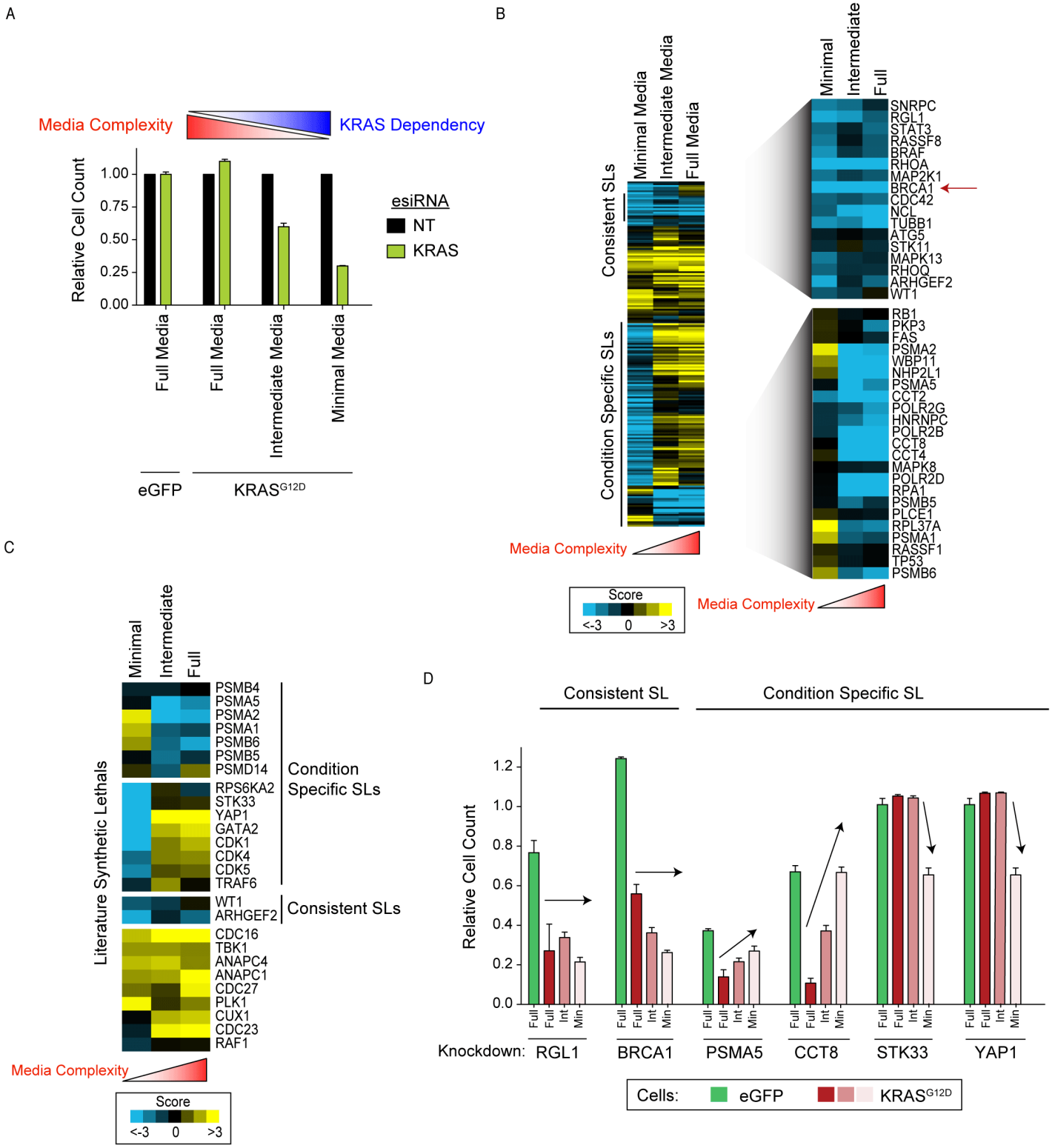
A
Media Complexity
KRAS Dependency
Relative Cell Count
1.00
0.75
0.50
0.25
0.00
esiRNA
NT
KRAS
Full Media
Full Media
Intermediate Media
Minimal Media
eGFP
KRAS G12D
B
Minimal Media
Intermediate Media
Full Media
Consistent SLs
Condition Specific SLs
Minimal
Intermediate
Full
SNRPC
RGL1
STAT3
RASSF8
BRAF
RHOA
MAP2K1
BRCA1
CDC42
NCL
TUBB1
ATG5
STK11
MAPK13
RHOQ
ARHGEF2
WT1
RB1
PKP3
FAS
PSMA2
WBP11
NHP2L1
PSMA5
CCT2
POLR2G
HNRNPC
POLR2B
CCT8
CCT4
MAPK8
POLR2D
RPA1
PSMB5
PLCE1
RPL37A
PSMA1
RASSF1
TP53
PSMB6
Media Complexity
Score
<-3
0
>3
Media Complexity
C
Minimal
Intermediate
Full
Literature Synthetic Lethals
PSMB4
PSMA5
PSMA2
PSMA1
PSMB6
PSMB5
PSMD14
RPS6KA2
STK33
YAP1
GATA2
CDK1
CDK4
CDK5
TRAF6
Condition Specific SLs
WT1
ARHGEF2
Consistent SLs
CDC16
TBK1
ANAPC4
ANAPC1
CDC27
PLK1
CUX1
CDC23
RAF1
Media Complexity
Score
<-3
0
>3
D
Consistent SL
Condition Specific SL
Relative Cell Count
1.2
1.0
0.8
0.6
0.4
0.2
0.0
Full
Full
Int
Min
Knockdown:
RGL1
BRCA1
PSMA5
CCT8
STK33
YAP1
Cells:
eGFP
KRAS G12D

**Figure 6**

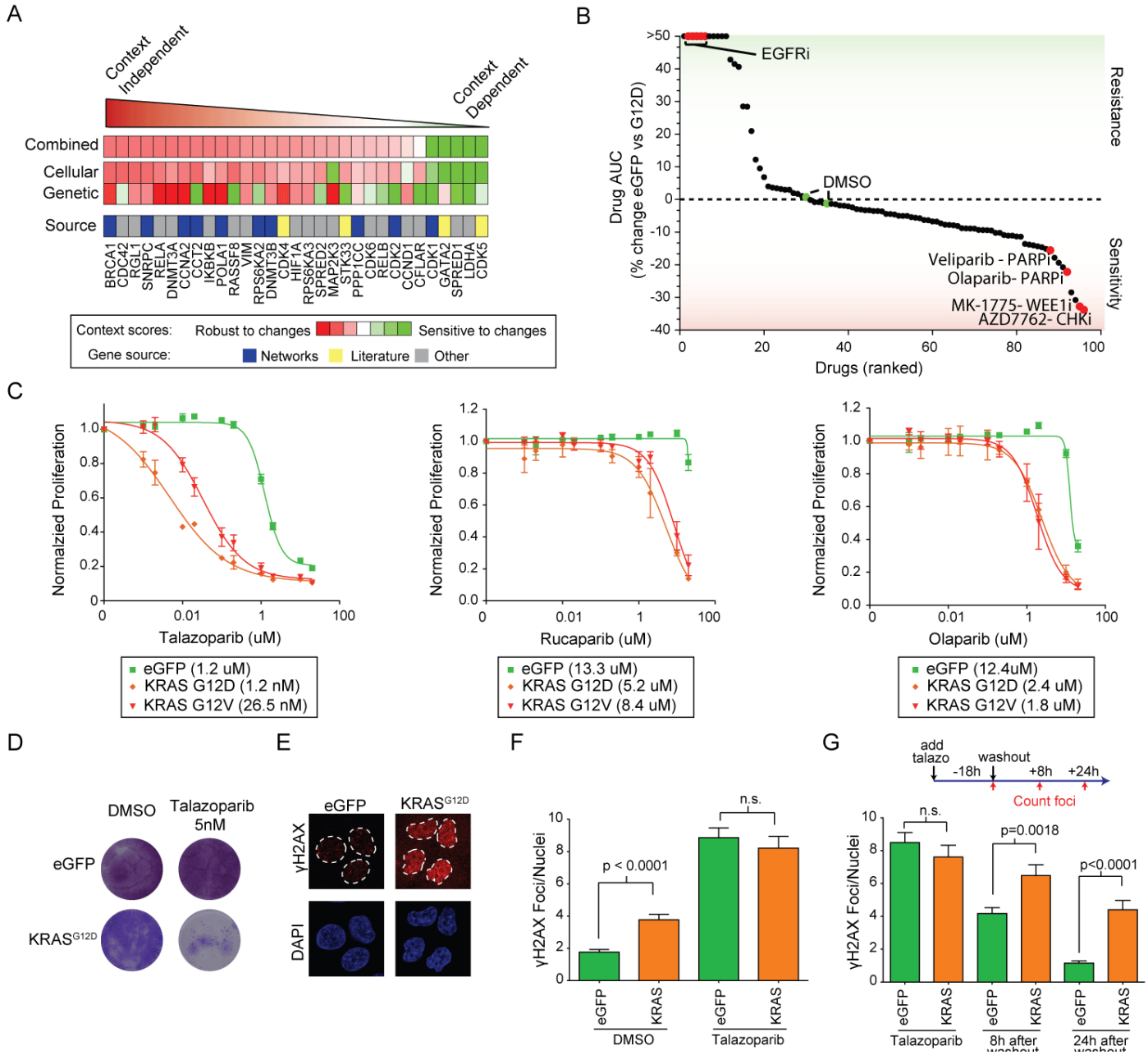
A
Context Independent
Context Dependent
Combined
Cellular
Genetic
Source
BRCA1 CDC42 RGL1 SNRPC RELA DNMT3A CCNA2 CCT2 IKBKB POLA1 RASSF8 VIM RPS6KA2 DNMT3B CDK4 HIF1A RPS6KA3 SPRED2 MAP2K3 STK33 PPP1CC CDK6 RELB CDK2 CCND1 CFLAR CDK1 GATA2 SPRED1 LDHA CDK5
Context scores: Robust to changes Sensitive to changes
Gene source: Networks Literature Other
B
EGFRi
DMSO
Veliparib - PARPi
Olaparib- PARPi
MK-1775- WEE1i
AZD7762- CHKi
Resistance
Sensitivity
Drug AUC (% change eGFP vs G12D)
Drugs (ranked)
C
Normalzied Proliferation
Talazoparib (uM)
eGFP (1.2 uM)
KRAS G12D (1.2 nM)
KRAS G12V (26.5 nM)
Rucaparib (uM)
eGFP (13.3 uM)
KRAS G12D (5.2 uM)
KRAS G12V (8.4 uM)
Olaparib (uM)
eGFP (12.4uM)
KRAS G12D (2.4 uM)
KRAS G12V (1.8 uM)
D
DMSO
Talazoparib 5nM
eGFP
KRAS G12D
E
eGFP
KRAS G12D
γH2AX
DAPI
F
γH2AX Foci/Nuclei
p < 0.0001
n.s.
eGFP
KRAS
DMSO
Talazoparib
G
add talazo
washout
-18h
+8h
+24h
Count foci
n.s.
p=0.0018
p<0.0001
Talazoparib
8h after washout
24h after washout